Gold Nanoparticles Induce Autophagosome Accumulation through Size-Dependent Nanoparticle Uptake and Lysosome Impairment

Xiaowei Ma,[†,∥] Yanyang Wu,[‡,∥] Shubin Jin,[†] Yuan Tian,[⊥] Xiaoning Zhang,[§] Yuliang Zhao,[†] Li Yu,[‡,*] and Xing-Jie Liang[†,*]

[†]Laboratory of Nanomedicine and Nanosafety, Division of Nanomedicine and Nanobiology, National Center for Nanoscience and Technology, China, and CAS Key Laboratory for Biomedical Effects of Nanomaterials and Nanosafety, Chinese Academy of Sciences, Beijing 100190, People's Republic of China, [‡]State Key Laboratory of Biomembrane and Membrane Biotechnology, School of Life Sciences, Tsinghua University, Beijing 100084, People's Republic of China, [§]Laboratory of Pharmaceutics, College of Medicine, Tsinghua University, Beijing 100084, People's Republic of China, and [⊥]College of Food Science and Nutritional Engineering, China Agricultural University, Beijing 100193, People's Republic of China. [∥]These authors contributed equally to this work.

ABSTRACT Development of nanotechnology calls for a comprehensive understanding of the impact of nanomaterials on biological systems. Autophagy is a lysosome-based degradative pathway which plays an essential role in maintaining cellular homeostasis. Previous studies have shown that nanoparticles from various sources can induce autophagosome accumulation in treated cells. However, the underlying mechanism is still not clear. Gold nanoparticles (AuNPs) are one of the most widely used nanomaterials and have been reported to induce autophagosome accumulation. In this study, we found that AuNPs can be taken into cells through endocytosis in a size-dependent manner. The internalized AuNPs eventually accumulate in lysosomes and cause impairment of lysosome degradation capacity through alkalinization of lysosomal pH. Consistent with previous studies, we found that AuNP treatment can induce autophagosome accumulation and processing of LC3, an autophagosome marker protein. However, degradation of the autophagy substrate p62 is blocked in AuNP-treated cells, which indicates that autophagosome accumulation results from blockade of autophagy flux, rather than induction of autophagy. Our data clarify the mechanism by which AuNPs induce autophagosome accumulation and reveal the effect of AuNPs on lysosomes. This work is significant to nanoparticle research because it illustrates how nanoparticles can potentially interrupt the autophagic pathway and has important implications for biomedical applications of nanoparticles.

KEYWORDS: gold nanoparticles (AuNPs) · autophagosome accumulation · autophagic flux · lysosome impairment · lysosomal pH

Autophagy is a lysosome-based degradative pathway which plays an essential role in maintaining cellular homeostasis. During autophagy, intracellular contents are engulfed by double-membrane vesicles named autophagosomes. Autophagosomes then fuse with lysosomes to form hybrid organelles named autolysosomes. The engulfed intracellular contents and inner membrane of autophagosomes are degraded inside autolysosomes.[1,2] Finally, autolysosomes are disassembled and lysosome components are retrieved through a newly identified cellular process named autophagic lysosome reformation.[3] Autophagy can be induced by various stimuli, including starvation, cytokines, caspase inhibition, and chemical reagents such as rapamycin.[4] In yeast, the major function of autophagy is to adjust the metabolic machinery in response to varying energy sources, thereby ensuring cell survival in an ever-changing environment.[5] In mammalian cells, however, the roles of autophagy are more complex. Autophagy has been implicated in cellular processes as varied as cell survival, cell death, pathogen clearance, and antigen presentation and has been linked to various diseases such as cancer and neuron degenerative diseases.[6]

Autophagy operates at two levels. Under nutrient-rich conditions, low-level basal autophagy is activated constitutively; however, due to the low rate of autophagosome formation under such conditions, autophagosomes are quickly turned over by lysosomes and therefore few or no autophagosomes are accumulated. Under stress conditions such as starvation, autophagy is actively induced, causing accumulation of autophagosomes through an elevated rate of autophagosome formation.[7] The most commonly used method to measure autophagy is based on monitoring autophagosome formation. During autophagy, microtubule-associated light chain 3 (LC3), a cytosolic protein under nutrient-rich conditions, is covalently conjugated to phosphatidylethanolamine (PE); PE-conjugated LC3 (named LC3-II)

* Address correspondence to liyulab@mail.tsinghua.edu.cn, liangxj@nanoctr.cn.

Received for review June 11, 2011 and accepted October 5, 2011.

Published online October 05, 2011
10.1021/nn202155y

then translocates to the autophagosome membrane. Therefore, microscopic analysis of the formation of LC3 punctate structures[8] and biochemical analysis of the conversion of LC3-I to LC3-II are widely used to monitor autophagosome formation.[9] Since the accumulation of autophagosomes can result from true induction of autophagy or blockade of autophagic flux (the turnover of autophagosomes by lysosomes[10]), additional measurements, for example, monitoring the degradation of an autophagy substrate such as p62, are required for establishing induction of autophagy.

Nanotechnology offers unique approaches to detect and modulate a variety of biomedical processes that occur at the nanometer scale and is expected to have a revolutionary impact on biology and medicine.[11,12] Nanoparticles, the size of which falls into the range of biological molecules and structures, have attracted much attention in recent years for their potential applications in biomedical research.[13] Useful properties can be incorporated into nanoparticles for manipulation or detection of biological structures and events.[14,15] Recently, various kinds of nanoparticles, including gold nanoparticles,[16] fullerene and its derivatives,[17−19] dendrimers,[20] quantum dots,[21,22] and neodymium oxides[23] were shown to induce autophagy, and nanoparticles were defined as a novel class of autophagy activators.[24] Our data clarify the mechanism of AuNP-induced autophagosome accumulation and might have important implications for developing nanoparticles for biomedical applications.

RESULTS AND DISCUSSION

Synthesis and Characterization of Gold Nanoparticles. Colloidal gold nanoparticles (AuNPs) were synthesized following the protocol described in the Methods section. AuNPs were demonstrated to have negative surface charges by dynamic light scattering (DLS), and the result was consistent with previous studies on NPs synthesized under the same conditions. AuNPs were stable in culture medium due to the electrostatic interaction of the surface charge of the nanoparticles. AuNPs with diameters around 10, 25, and 50 nm were characterized with transmission electron microscopy (TEM) (Figure 1A), which indicates consistent size. The hydrated diameter of the AuNPs was confirmed by DLS measurement (Figure 1B). The synthesized AuNPs were analyzed using UV−vis absorbance spectrophotometry. The plasmon absorption is clearly visible, and its maximum red shifts with increasing particle diameter (λ_{max} = 517, 522, and 535 nm for the 10, 25, and 50 nm particles) (Figure S1 in Supporting Information).

Cellular Uptake of Gold Nanoparticles Is Size-Dependent. To explore the relation between the size of AuNPs and cellular uptake efficiency, normal rat kidney (NRK) cells were treated with AuNPs of different sizes for 24 h and examined by optical microscopy and TEM. Recent research shows that the uptake of nanoparticles by the cell is strongly dependent upon particle size.[25,26] The cellular uptake of gold nanoparticles between 10 and 50 nm in diameter has an increasing trend, with maximum uptake by a cell occurring at a nanoparticle size of 50 nm.[27−29] It has been previously reported that the uptake of AuNPs is mediated by nonspecific adsorption of serum proteins onto the gold surface, and AuNPs are taken up into the cells *via* the receptor-mediated endocytosis pathway. Since serum proteins contain a diverse set of proteins, the surface of the citrate-stabilized AuNPs probably contains a variety of serum proteins on its surface. The presence of these proteins on the surface of the nanoparticles is related to the particle's size and dictates the uptake amount. From a kinetic point of view, cellular uptake of AuNPs is also affected by thermodynamic driving force for wrapping. For the smaller NPs to go in, increased elastic energy associated with bending of the membrane results in decreased driving force for membrane wrapping of the particle. Hence, smaller particles must be clustered together to create enough driving for uptake; therefore, the uptake amount is much smaller than 50 nm AuNPs.[30,31] In our experiment, we used AuNPs synthesized using the same method (citrate reduction of chloroauric acid) described previously.[27] There were no obvious morphological alterations and discernible effect on longevity of cells treated with AuNPs. However, microscopic analysis reveals that the cellular uptake of AuNPs is size-dependent, with larger AuNPs more readily taken up by cells (Figure 1C). TEM analysis indicates a similar size-dependent cellular uptake of AuNPs (Figure 1E). To quantify the relation between the size of AuNPs and cellular uptake efficiency, a quantitative inductively coupled plasma mass spectrometry (ICP-MS) measurement was conducted, which estimates the amount of AuNPs internalized by cells. The concentration of gold atoms in acid-digested cell solutions was directly measured with ICP-MS. The number of AuNPs per cell was calculated according to the number of atoms in each AuNP and the number of cells in the solution.[27] Figure 1D shows a histogram of the number of AuNPs per cell *versus* the size of AuNPs. It indicates that cellular uptake of AuNPs is heavily dependent upon particle size, with 50 nm AuNPs most readily internalized by cells, followed by 25 nm AuNPs and 10 nm AuNPs.

Gold-Nanoparticle-Induced Autophagosome Accumulation Is Size-Dependent. Previous studies have shown that AuNPs can induce autophagy.[16] Using a NRK cell line which stably expresses cyan fluorescent protein (CFP)-tagged LC3 (LC3-CFP), we found that AuNPs can indeed induce accumulation of LC3-positive punctuate structures (Figure 2A). Western blot analysis showed an increased LC3-II/LC3-I ratio (Figure 2B,C), which further confirms autophagosome accumulation in AuNP-treated cells. Interestingly, the AuNP-induced autophagosome

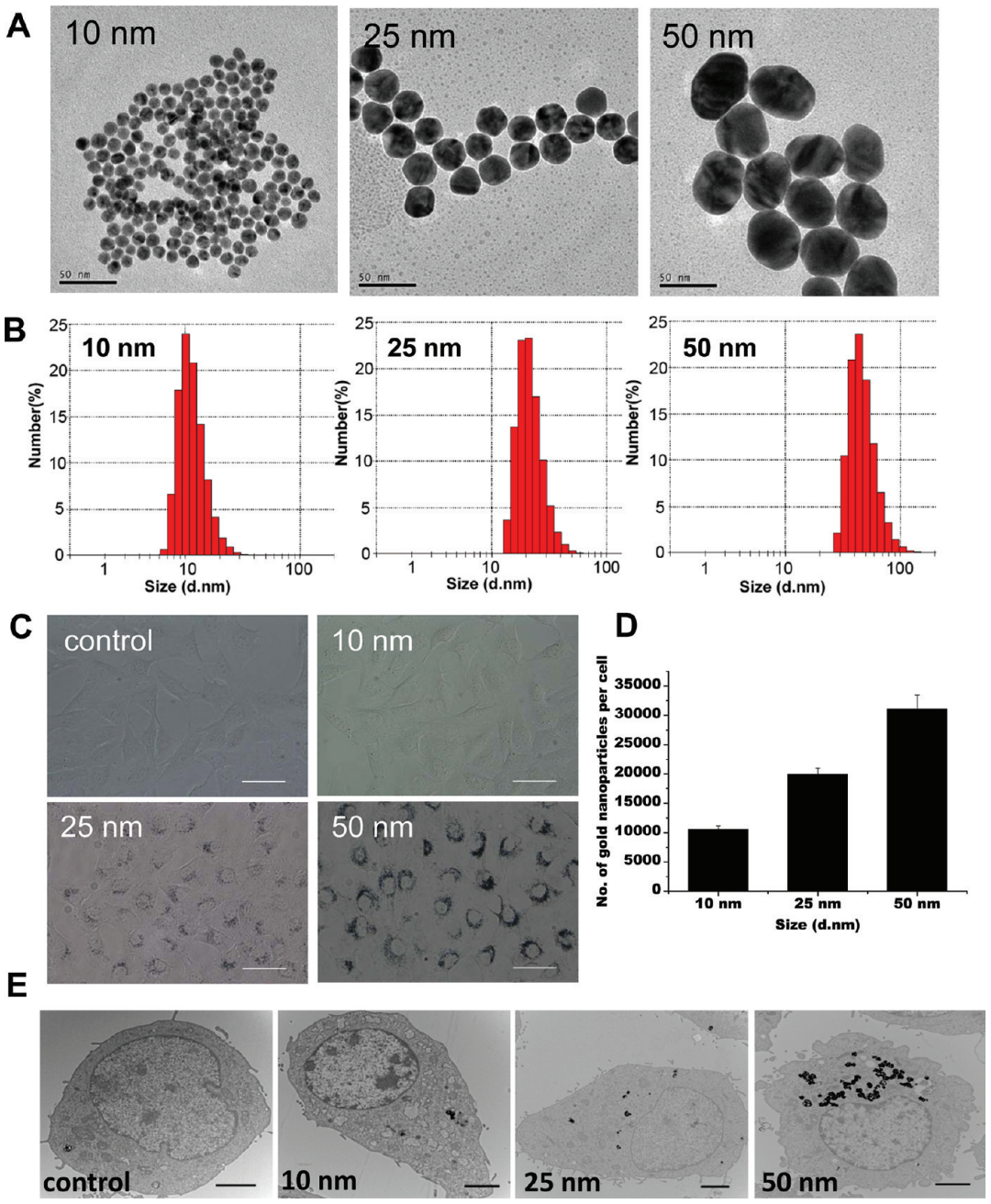

Figure 1. Characterization of AuNPs. (A) AuNPs characterized by TEM (scale bar, 50 nm). (B) Size of AuNPs, as measured by dynamic light scattering (DLS). (C) AuNPs form distinct dark aggregates in cells. Representative bright-field images are shown of NRK cells untreated (control) or treated with AuNPs of 10, 25, and 50 nm in diameter for 24 h (scale bar, 50 μm). (D) Size-dependent cellular uptake of AuNPs. The graph shows the number of AuNPs per cell after incubation with 1 nM AuNPs for 24 h. (E) TEM images of NRK cells untreated (control) or treated with AuNPs with diameters of 10, 25, and 50 nm. The AuNPs are internalized by cells and trapped inside lysosomes (scale bar, 2 μm).

accumulation is size-dependent, with larger AuNPs causing accumulation of more autophagosomes in the cell. The ratio of LC3-II/LC3-I in Figure 2C was measured by integrated optical densitometry (IOD) and showed that the LC3-II/LC3-I ratio increased from 0.78 to 1.02 (10 and 25 nm, respectively) and to 1.12 (50 nm).

Gold Nanoparticle Treatment Blocks Autophagic Flux and Degradation of an Autophagy Substrate. Autophagosome accumulation can result from either autophagy induction or the blockade of autophagic flux. To distinguish between these possibilities, we carried out an "autophagic flux assay". This is based on the observation that LC3-II is degraded in autolysosomes, so the total amount of LC3-II is determined by the balance between LC3-II production and degradation. However, when lysosomal degradation is inhibited, the amount of LC3-II is strictly dependent on LC3-II production. Therefore, by comparing the amount of LC3-II in the presence and absence of a lysosome degradation

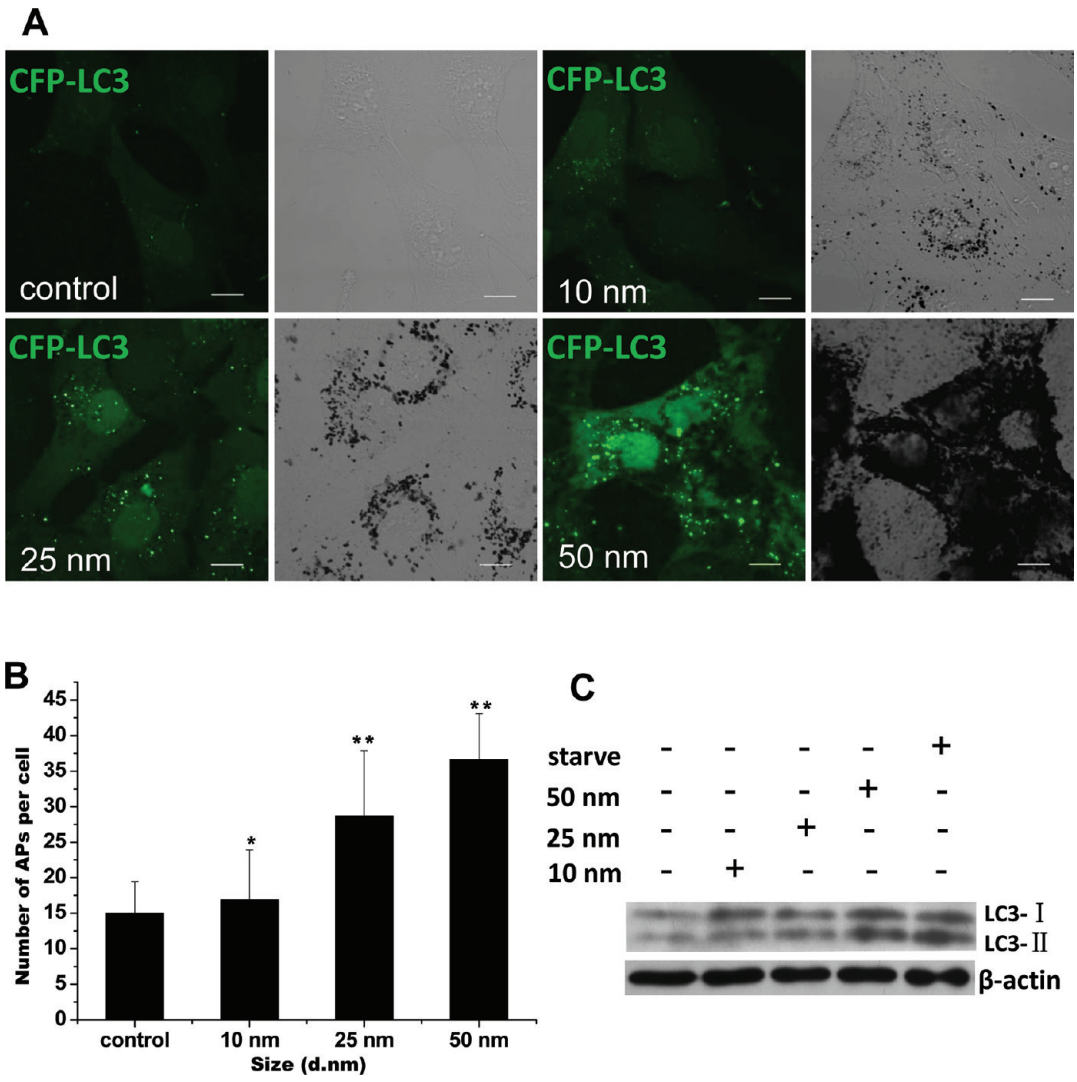

Figure 2. Induction of LC3 puncta by AuNP treatment. (A) Formation of CFP-LC3 dots (pseudocolored as green) in CFP-LC3 NRK cells treated for 24 h with 1 nM AuNPs of the sizes indicated. Left, confocal image; right, bright-field image (scale bar, 10 μm). (B) Statistical analysis of the number of autophagosomes (APs) per cell after 24 h of treatment. (C) Conversion of LC3 from the cytoplasmic form (LC-I) to the autophagosome-associated form (LC3-II). Cells either cultured in nutrient-rich medium for 24 h or cultured under starvation conditions (depletion of both amino acids and serum) for 5 h, or treated with 1 nM AuNPs of the sizes indicated for 24 h, were harvested and subjected to Western blotting analysis with anti-LC3 antibody. β-Actin served as loading control. AP: autophagosome.

inhibitor, we can determine whether or not autophagy is, in fact, induced.[32] Starvation is the stimulus most widely used to induce autophagy, and we found that starvation causes LC3-II accumulation as expected (Figure 3A,B). Adding the lysosome degradation inhibitor chloroquine further increases the starvation-induced accumulation of LC3-II. However, there is no increase of LC3-II level in cells cotreated with AuNPs and chloroquine, indicating that AuNPs do not actually induce autophagy.

To further confirm our conclusion that nanoparticle treatment does not induce autophagy, autophagic degradation was monitored by measuring p62 (also known as SQSTM1/sequestome1), a substrate that is preferentially degraded by autophagy.[33] We found that starvation caused rapid degradation of p62, and the presence of a lysosome degradation inhibitor potently blocked starvation-induced p62 degradation. However, AuNP treatment did not cause p62 degradation but instead caused accumulation of p62, which indicates possible impairment of autophagic degradation capacity (Figure 3C,D). From these results, we conclude that AuNP treatment causes autophagosome accumulation through blockade of autophagic flux.

Several signaling pathways regulate autophagy in mammalian cells. The classical pathway involves the inhibition of a serine/threonine protein kinase, called mTOR (mammalian target of rapamycin) during autophagy induction. It has been reported that nanoparticles can induce autophagy by modulating the activity of mTOR, the master regulator of autophagy.[20] We used phospho-p70 S6 kinase (P-S6K) as

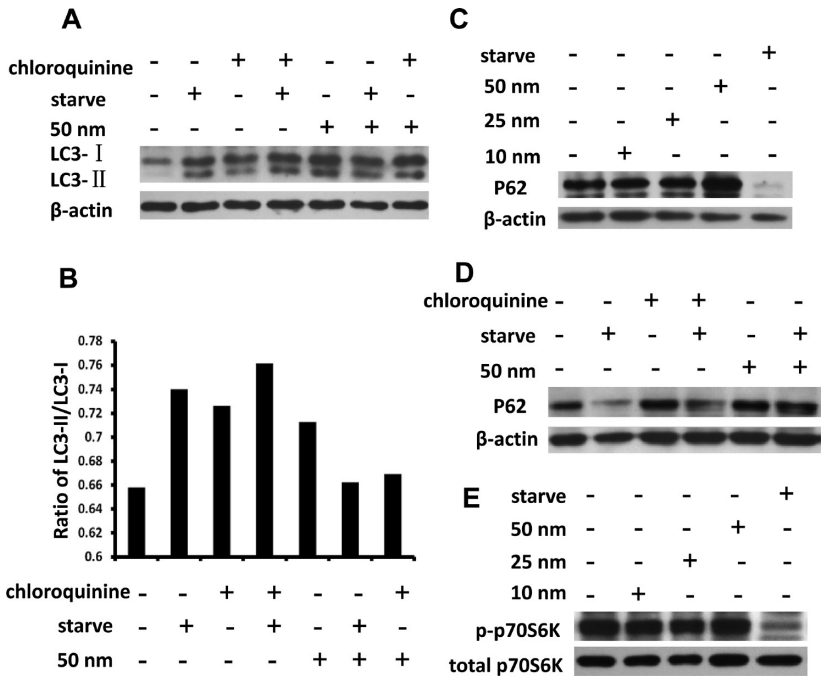

Figure 3. Autophagic flux detection. (A) LC3 turnover assay. Cells were cultured as follows: in regular culture medium for 24 h (lane 1); under starvation conditions for 5 h (lane 2); in regular culture medium containing 20 μM chloroquine for 1 h (lane 3); with chloroquine under starvation conditions (lane 4); in DMEM containing 1 nM 50 nm AuNPs for 24 h (lane 5); in DMEM containing 1 nM 50 nm AuNPs for 24 h then starved for 5 h (lane 6); with chloroquine and 50 nm AuNPs (lane 7). The differences in LC-I and LC3-II levels were compared by immunoblot analysis of cell lysates with an anti-LC3 antibody. The positions of LC3-I and LC3-II are indicated. β-Actin served as loading control. (B) Comparison of the ratio of LC3-II/LC3-I, measured by integrated optical densitometry (IOD), in samples cultured as in (A). (C) Degradation of the autophagy-specific substrate p62. Cells starved or treated with AuNPs for 24 h were harvested and subjected to Western blot analysis using anti-p62 antibody and anti-β-actin antibody. (D) Cells were cultured as in (A), and degradation of p62 was detected by immunoblotting. β-Actin served as loading control. (E) Effect of AuNPs on the mTOR signaling pathway. Cells starved or treated with AuNPs for 24 h were Western blotted with anti-p70S6K and antiphospho-p70S6K antibodies.

a marker for mTOR activity. We found that, whereas P-S6K is greatly lost after starvation, AuNP treatment had no effect on mTOR activity (Figure 3E). This result further supports our conclusion that AuNPs cause autophagosome accumulation through blockade of autophagic flux.

Gold Nanoparticles Cause Impairment of Autophagosome/Lysosome Fusion and Lysosome Enlargement. AuNPs could block autophagic flux by affecting fusion between autophagosomes and lysosomes or by lowering the degradation capacity of lysosomes. To test between these alternatives, we treated NRK cells stably expressing the lysosome marker red fluorescent protein (RFP)-tagged lamp 1 (Lamp1-RFP) and the autophagosome marker LC3-CFP with AuNPs for 24 h. Lamp 1, lysosomal-associated membrane protein 1, is a highly abundant glycoprotein in lysosomal membranes. AuNP treatment caused impaired fusion between autophagosomes and lysosomes (Figures S2A,B in Supporting Information). Interestingly, both confocal microscopy images (Figure 4A,B) and TEM pictures (Figure 4C) show enlarged lysosomes in the AuNP-treated cells. It is well-established that defective lysosome degradation can cause lysosome enlargement.[34] Therefore, we speculate that the accumulation of AuNPs inside lysosomes may compromise the degradation capacity of lysosomes and thus cause lysosome enlargement.

Gold Nanoparticle Treatment Causes Impairment of Lysosome Degradation Capacity. To test whether lysosome degradation capacity is impaired after AuNP treatment, we labeled cells with derivative-quenched bovine serum albumin, DQ-BSA, a self-quenched lysosome degradation indicator.[35] Lysosomal degradation of DQ-BSA results in release of nonquenched protein fragments that are brightly fluorescent. As shown in Figure 4D,E, AuNP treatment caused significant impairment of lysosome degradation capacity. We noticed that there was a correlation between the size of AuNPs and the degree of lysosome impairment. To further test the effect of AuNPs on lysosomes, we measured the activity of a lysosome marker enzyme, acid phosphatase, and found that its activity was significantly lower in AuNP-treated cells (Figure 4F). On the basis of these data, we conclude that AuNP treatment causes impairment of lysosome degradation capacity. To explore the effects of AuNPs on endosomes, we also treated NRK cells expressing the endosomal membrane identity marker red fluorescent protein (RFP)-tagged Rab7 with AuNPs for 24 h. Rab7 is a member of the Ras superfamily of small Rab GTPases that locate in late

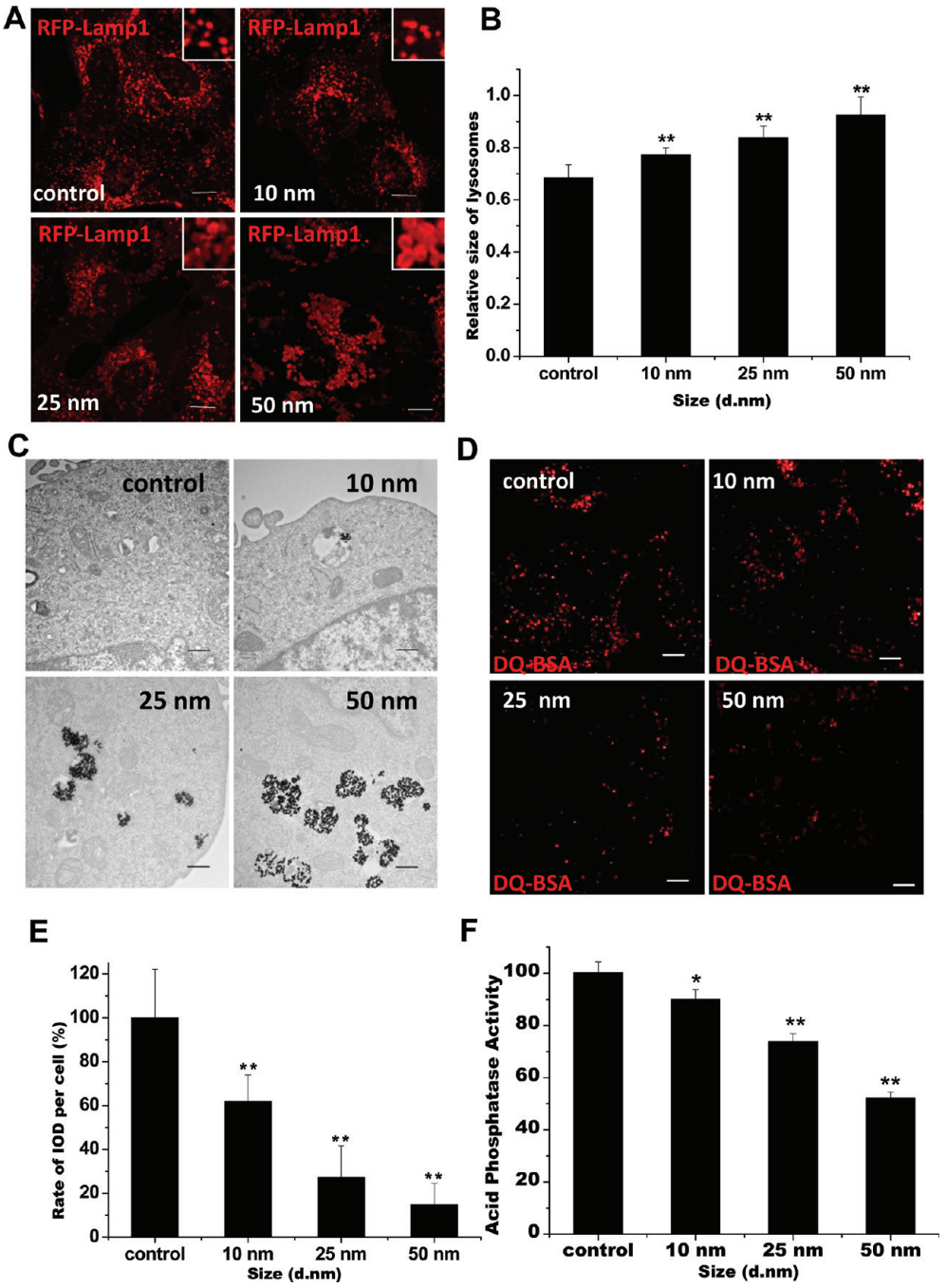

Figure 4. Impairment of lysosomes by AuNPs. (A) Vacuoles induced by AuNP treatment are enlarged lysosomes. NRK cells were incubated for 24 h with plain medium (control) or with 1 nM AuNPs. Inset: close-up of the enlarged lysosomes (scale bar, 10 μm). (B) Lysosomal size was analyzed with Image pro-plus 6.0 software. The number of lysosomes analyzed was as follows: control, n = 7437; 10 nm, n = 7726; 25 nm, n = 8548; 50 nm, n = 4564. (C) TEM pictures of enlarged lysosomes after AuNP treatment (scale bar, 500 nm). (D) DQ-BSA analysis of lysosomal proteolytic activity. Accumulation of fluorescent signal, generated from lysosomal proteolysis of DQ-BSA, was much lower in AuNP-treated cells (scale bar, 10 μm). (E) Fluorescence intensity of the brightly fluorescent fragments released by lysosomal degradation of DQ-BSA was quantified by densitometry (IOD). At least 40 cells were analyzed for each treatment. There was a statistically significant difference in lysosomal proteolytic activity between the control cells and cells treated with AuNPs. (F) Acid phosphatase enzyme activity measurement of NRK cells treated with AuNPs for 24 h.

endosomes. Confocal microscopy images show enlarged endosomes after AuNP treatment, indicating that AuNPs not only affect the terminal of the endocytic pathway but also affect endosomes (Figure S3 in Supporting Information).

Gold Nanoparticle Treatment Causes Lysosome Alkalinization. Most lysosomal enzymes have an optimal pH of 4.5.[36] Many lysosome inhibitors affect lysosome function by altering lysosome pH.[37−39] Chloroquine as lysosomal inhibitor can increase the lysosome pH[40] and cause

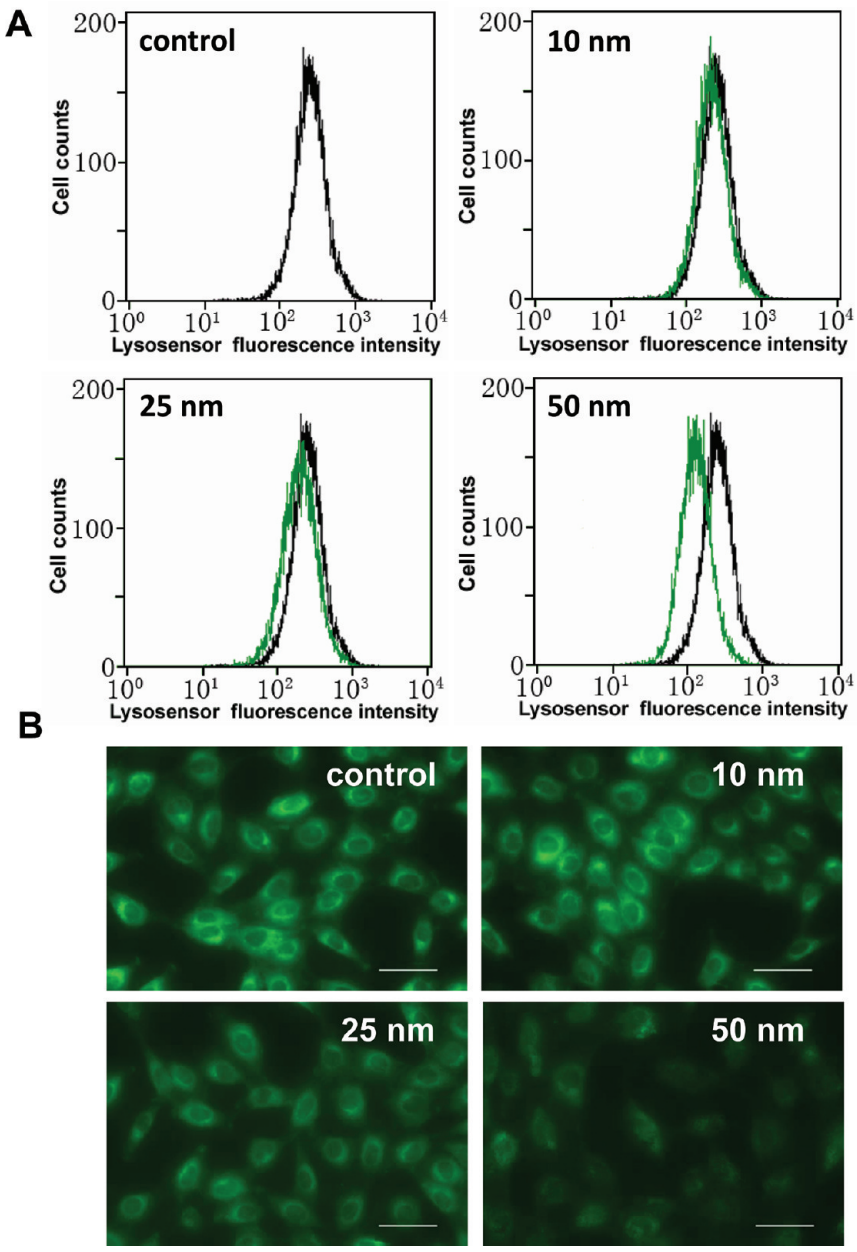

Figure 5. Effect of AuNPs on lysosome pH. (A) FACS analysis of cells stained with LysoSensor Green DND-189. The effect of 10, 25, and 50 nm AuNP treatment on lysosome pH was analyzed 24 h after treatment. Black line, control cells; green line, AuNP-treated cells. (B) Representative fluorescent pictures of NRK cells treated with AuNPs for 24 h, then exposed for 30 min to 1 μmol/L LysoSensor Green DND-189 (scale bar, 50 μm).

accumulation of autophagosomes in the cytoplasm and impaired fusion between autophagosomes and lysosomes (Figure S4).

LysoSensor Green DND-189 is an acidotropic dye that accumulates in intracellular acidic organelles as the result of protonation and has a fluorescence intensity that is proportional to acidity. Previous characterization of LysoSensor Green DND-189 showed a well-defined pH-dependent increase in fluorescence intensity in response to acidifying change of the organelle pH.[41,42] To test whether AuNPs can affect lysosome pH, in our experiment, the cells were labeled with LysoSensor Green DND-189 dye for comparison of lysosome acidity. Flow cytometry analysis showed size-dependent alkalinization of lysosomes in AuNP-treated cells (Figure 5A). Fluorescent microscopic analysis confirmed this effect (Figure 5B). Taken together, our data show that AuNP treatment causes alkalinization of lysosomes. Lysosome acidification is regulated by the vacuolar H+(V)-ATPase, composed of a membrane-associated ion conductance Vo protein complex and a peripherally associated ATPase V1 protein complex. The reversible dissociation of the V1 protein from the Vo protein down-regulates the V-ATPase activity.[43,44] In the untreated cells, the V1 protein was localized on lysosome with a punctuated localization staining

pattern. However, upon AuNP treatment, we found the localization pattern of V1 protein became increasingly diffused in a AuNP size-dependent manner, indicating the dissociation of the V1 protein from the lysosome bound Vo protein (Figure S5). From these data, we conclude that AuNPs cause lysosome alkalinization through dissociating V1 protein from the lysosome-resident Vo protein of vacuolar H+(V)-ATPase.

Autophagy operates at two levels. Under nutrient-rich conditions, low-level basal autophagy is activated constitutively; however, autophagosomes do not accumulate because they are formed at a low rate and are quickly turned over by lysosomes. When cells are stressed, such as during starvation, autophagy is actively induced and the rate of autophagosome formation is elevated, causing accumulation of autophagosomes. Therefore, accumulation of autophagosomes, or elevated levels of the autophagosome marker LC3-II, is necessary but not sufficient to conclude that a certain stimulus can induce autophagy.

Autophagy has been shown to play important roles in modulating many important physiological functions such as cell survival under stress conditions,[45] cell death,[46] and organelle quality control.[47] However, the primary function of autophagy is degradation, and autophagy modulates other physiological functions through degradation.[48] From the standpoint of degradation, autophagy induction and basal autophagy blockade have opposite effects; the former enhances intracellular degradation, while the latter inhibits it. Therefore, autophagy induction and basal autophagy blockade have very different physiological consequences.

In recent years, much effort has been made to develop therapeutic approaches based on modulating autophagy. Researchers are particularly interested in compounds which can activate autophagy to treat conditions such as neurodegenerative diseases.[49] Various nanoparticles have been reported to induce autophagosome accumulation and proposed as autophagy activators and thus have been considered to have therapeutic potential. Colloidal gold nanoparticles have great potential for disease therapy in the clinic because of their biocompatibility, small size, and tunable surface functionalities.[50,51] Multiple lines of evidence in our study establish that accumulation of autophagosomes in AuNP-treated cells does not result from autophagy induction but is caused by blockade of basal autophagy. Nanoparticles, such as gold nanoparticles, fullerene and its derivatives, dendrimers, quantum dots, and neodymium oxide have all been shown to induce autophagy, and nanoparticles were defined as a novel class of autophagy activator.[24] Owing to the similarity of AuNPs with these nanoparticles, we have to be cautious about using nanoparticles as autophagy activators in light of our results.

Lysosomes are major intracellular degradation organelles. Defects in lysosome function have serious physiological and pathological consequences. For example, lysosome storage diseases, a group of approximately 50 rare inherited metabolic disorders, result from defects in lysosomal function.[52] AuNPs enter the cell through endocytosis, and when they reach the terminus of the endocytic pathway, they accumulate in lysosomes and impair lysosome function. The ultrasmall size of nanomaterials offers great possibilities for their usage in biomedical research. They can potentially carry drugs to the target tissues, image the targeted tissues, and release their cargo in response to signals or upon reaching appropriate cellular compartments.[53,54] However, the unique physiochemical properties that make nanomaterials so attractive for pharmaceutical and clinical applications may also be associated with their potential toxicity hazards.[55,56] Therefore, it could lead to a better understanding of nanoparticle toxicity by deeply elucidating the metabolism of NPs in cells. In addition to clarifying the mechanism by which AuNPs induce autophagosome accumulation and lysosome impairment, the findings from our study will provide some guidance in the rational design and synthesis of nanoparticles for biomedical applications. For example, the rate of autophagosome turnover could be monitored by choosing appropriate nanoparticles as autophagy modulators, and the cellular metabolism could be adjusted with designing nanostructures for more efficient and safer imaging and therapeutic applications with least effect on the normal cellular physiological activities. Nanoparticle size is an important determinant of physicochemical properties and biomedical behaviors. The size of most nanoparticles used in biomedical research allows them to get into cells through endocytosis; hence they may inflict similar damage to lysosomes and impair the overall cellular degradation capacity. Although a wide spectrum of biomedical applications of nanomaterials have been proposed, significant clinical applications are limited with polymeric materials such as polymer particles[57] and liposomal preparations,[58] which are generally larger than 100 nm. Biomedical applications of engineered nanoparticles such as AuNPs, with greater size and shape variabilities than liposomes and polymers, are being actively pursued. AuNPs ranging from 10 to 50 nm are widely used for cell imaging, targeted drug delivery, and cancer diagnostics and therapeutic applications. These studies are representative of the initial applications of nanoparticles in biology and medicine. It is important to investigate the intracellular behavior of nanoparticles within this size range. In our study, we have chosen three representative sizes (10, 25, and 50 nm) to demonstrate their bioactivities. Investigations are still needed in further studies on the effect of other particle size ranges and additional parameters (such as shape and surface fictionalization *etc.*) on the autophagosome accumulation. We have some preliminary results on differently charged 50 nm

AuNPs. We found positively charged AuNP treatment can also block the autophagic pathway by accumulating in the lysosomes and impairing the lysosomes. Positively charged 50 nm AuNPs caused accumulation of more autophagosomes in the cell and more significant enlargement of lysosomes as compared with negatively charged 50 nm Au NPs (Figure S6 in Supporting Information).

Further careful validation of the possible effects of nanoparticles on cells is required before they can be applied in clinics. One important implication of our finding is that we have to take their potential disturbance to the lysosome and autophagic pathway into consideration when we use them in therapeutic-related applications.

METHODS

AuNP Synthesis and Preparation. The 25 and 50 nm diameter colloidal gold nanoparticles were prepared according to the method developed by Frens.[59] Briefly, 400 μL of 1% chloroauric acid was added to 40 mL of Milli-Q water (18 MΩ cm^{-1}), and the solution was heated to boiling. Next, 800 and 360 μL of 1% citric acid were added to the solution to synthesize 25 and 50 nm AuNPs, respectively. Refluxing of the solution continued until the color of the boiling solution changed from dark blue to red wine color while stirring vigorously. AuNPs with a diameter of 10 nm were prepared by reversing the order of addition of chloroauric acid and sodium citrate.[60] Sodium citrate (68 mg) in 105 mL of Milli-Q water (18 MΩ cm^{-1}) was boiled, and then 1 mL of aqueous solution containing 9.5 mg of chloroauric acid was added. Boiling was then continued for 15 min and then left to cool to room temperature while stirring vigorously. Before treating the cells, the citrate buffer was removed by centrifugation and the AuNPs were resuspended in culture medium. All of these AuNPs have negative zeta-potential as measured by DLS.

Live Cell Imaging. The CFP-LC3 and Lamp1-RFP stable cell lines were seeded in Lab-Tek chambered cover glasses (Nunc, Rochester, NY, USA) overnight at 37 °C with 5% CO_2 in an incubator (Pecon) for microscopy. Images were digitally acquired by a confocal microscope (Olympus FV1000) and analyzed using instrument software Image pro-plus 6.0.

Electron Microscopy Analysis. Cells were trypsinized and then fixed in 2.5% glutaraldehyde in PBS (pH 7.4) for 10 min at room temperature. The fixed cells were then embedded in Lecia EM UC6, sectioned, and double stained with uranyl acetate and lead citrate for observation under the transmission electron microscope (H-7650B).

Acid Phosphatase Assay. After 24 h of culturing in growth media with or without AuNPs, cells were trypsinized and collected by centrifugation. Cells were washed and suspended in extraction buffer (from a lysosome isolation kit (LYSISO1), Sigma) before being broken open by sonication on ice. The samples were centrifuged to remove AuNPs. The supernatant liquid containing lysosomes and lysosomal enzymes was then tested for acid phosphatase activity using an acid phosphatase assay kit (Sigma).

Evaluation of Lysosomal Acidity. NRK cells were collected from growth media after treating with AuNPs for 24 h and washed twice in PBS. The cells were incubated for 30 min under growth conditions with 500 μL of prewarmed medium containing 2 μmol/L LysoSensor Green DND-189 dye. After washing, the cells were resuspended with PBS and immediately analyzed by flow cytometry (FACS). FL1 (green) fluorescence was collected within 1 min on a population of 20 000 cells.

Western Blotting. Cells were lysed in 2% SDS, and the samples were separated by SDS-PAGE before transferring to polyvinylidene difluoride membrane. Membranes were blocked in 5% nonfat milk and washed in Tris-buffered saline containing 0.1% Tween. Membranes were incubated with primary antibody and then the corresponding secondary antibody with three washing steps between.

DQ-BSA Assay. After 24 h of AuNP treatment, NRK cells were washed twice with PBS and then incubated in DMEM containing DQ Red BSA (D-12051, Molecular Probes) at a final concentration of 10 μg/mL for 3 h at 37 °C. Cells were then washed twice with PBS to remove excess probe and imaged by confocal microscopy.

Statistics. Differences between groups were analyzed by Student's *t* test (*different from control, $P < 0.05$; **different from control, $P < 0.01$). Results were expressed as means ± SEM. Images are representative of three or more experiments.

Acknowledgment. This work was supported in part by Chinese Natural Science Foundation project (No. 30970784), National Key Basic Research Program of China (2009CB930200), Chinese Academy of Sciences (CAS) "Hundred Talents Program" (07165111ZX), and CAS Knowledge Innovation Program.

Supporting Information Available: The methods and experimental procedures, UV−vis spectrophotometry characterization of AuNPs, confocal microscope images of NRK cells stably expressing both Lamp1-RFP (red) and LC3-CFP (pseudocolored as green) after AuNP treatment, confocal microscope images of NRK cells expressing Rab7-RFP (red) after AuNP treatment, confocal microscope images of NRK cells stably expressing both Lamp1-RFP (red) and LC3-CFP (pseudocolored as green) after chloroquine treatment, and the localization pattern change of V-ATPase upon AuNP treatment. This material is available free of charge *via* the Internet at http://pubs.acs.org.

REFERENCES AND NOTES

1. Mizushima, N. Autophagy: Process and Function. *Genes Dev.* **2007**, *21*, 2861–2873.
2. Xie, Z.; Klionsky, D. J. Autophagosome Formation: Core Machinery and Adaptations. *Nat. Cell Biol.* **2007**, *9*, 1102–1109.
3. Yu, L.; McPhee, C. K.; Zheng, L.; Mardones, G. A.; Rong, Y.; Peng, J.; Mi, N.; Zhao, Y.; Liu, Z.; Wan, F.; *et al.* Termination of Autophagy and Reformation of Lysosomes Regulated by MTOR. *Nature* **2010**, *465*, 942–946.
4. Azad, M. B.; Chen, Y.; Gibson, S. B. Regulation of Autophagy by Reactive Oxygen Species (ROS): Implications for Cancer Progression and Treatment. *Antioxid. Redox Signaling* **2009**, *11*, 777–790.
5. Abeliovich, H.; Klionsky, D. J. Autophagy in Yeast: Mechanistic Insights and Physiological Function. *Microbiol. Mol. Biol. Rev.* **2001**, *65*, 463–479.
6. Mizushima, N.; Levine, B.; Cuervo, A. M.; Klionsky, D. J. Autophagy Fights Disease through Cellular Self-Digestion. *Nature* **2008**, *451*, 1069–1075.
7. Codogno, P.; Meijer, A. J. Autophagy and Signaling: Their Role in Cell Survival and Cell Death. *Cell Death Differ.* **2005**, *12*, 1509–1518.
8. Takahashi, Y.; Coppola, D.; Matsushita, N.; Cualing, H. D.; Sun, M.; Sato, Y.; Liang, C.; Jung, J. U.; Cheng, J. Q.; Mule, J. J.; *et al.* Bif-1 Interacts with Beclin 1 through UVRAG and Regulates Autophagy and Tumorigenesis. *Nat. Cell Biol.* **2007**, *9*, 1142–1151.
9. Kabeya, Y.; Mizushima, N.; Ueno, T.; Yamamoto, A.; Kirisako, T.; Noda, T.; Kominami, E.; Ohsumi, Y.; Yoshimori, T. LC3, a Mammalian Homologue of Yeast Apg8p, Is Localized in Autophagosome Membranes after Processing. *EMBO J.* **2000**, *19*, 5720–5728.
10. Mizushima, N.; Yoshimori, T.; Levine, B. Methods in Mammalian Autophagy Research. *Cell* **2010**, *140*, 313–326.
11. Fu, C. C.; Lee, H. Y.; Chen, K.; Lim, T. S.; Wu, H. Y.; Lin, P. K.; Wei, P. K.; Tsao, P. H.; Chang, H. C.; Fann, W. Characterization and Application of Single Fluorescent Nanodiamonds

as Cellular Biomarkers. *Proc. Natl. Acad. Sci. U.S.A.* **2007**, *104*, 727–732.
12. Liang, X. J.; Meng, H.; Wang, Y.; He, H.; Meng, J.; Lu, J.; Wang, P. C.; Zhao, Y.; Gao, X.; Sun, B.; *et al.* Metallofullerene Nanoparticles Circumvent Tumor Resistance to Cisplatin by Reactivating Endocytosis. *Proc. Natl. Acad. Sci. U.S.A.* **2010**, *107*, 7449–7454.
13. Gao, J.; Gu, H.; Xu, B. Multifunctional Magnetic Nanoparticles: Design, Synthesis, and Biomedical Applications. *Acc. Chem. Res.* **2009**, *42*, 1097–1107.
14. Hwang do, W.; Song, I. C.; Lee, D. S.; Kim, S. Smart Magnetic Fluorescent Nanoparticle Imaging Probes To Monitor MicroRNAs. *Small* **2009**, *6*, 81–88.
15. Park, J. W.; Park, A. Y.; Lee, S.; Yu, N. K.; Lee, S. H.; Kaang, B. K. Detection of TrkB Receptors Distributed in Cultured Hippocampal Neurons through Bioconjugation between Highly Luminescent (Quantum Dot-Neutravidin) and (Biotinylated Anti-TrkB Antibody) on Neurons by Combined Atomic Force Microscope and Confocal Laser Scanning Microscope. *Bioconjugate Chem.* **2010**, *21*, 597–603.
16. Li, J. J.; Hartono, D.; Ong, C. N.; Bay, B. H.; Yung, L. Y. Autophagy and Oxidative Stress Associated with Gold Nanoparticles. *Biomaterials* **2010**, *31*, 5996–6003.
17. Wei, P.; Zhang, L.; Lu, Y.; Man, N.; Wen, L. C60(Nd) Nanoparticles Enhance Chemotherapeutic Susceptibility of Cancer Cells by Modulation of Autophagy. *Nanotechnology* **2010**, *21*, 495101.
18. Yamawaki, H.; Iwai, N. Cytotoxicity of Water-Soluble Fullerene in Vascular Endothelial Cells. *Am. J. Physiol. Cell Physiol.* **2006**, *290*, C1495–1502.
19. Zhang, Q.; Yang, W.; Man, N.; Zheng, F.; Shen, Y.; Sun, K.; Li, Y.; Wen, L. P. Autophagy-Mediated Chemosensitization in Cancer Cells by Fullerene C60 Nanocrystal. *Autophagy* **2009**, *5*, 1107–1117.
20. Li, C.; Liu, H.; Sun, Y.; Wang, H.; Guo, F.; Rao, S.; Deng, J.; Zhang, Y.; Miao, Y.; Guo, C.; *et al.* PAMAM Nanoparticles Promote Acute Lung Injury by Inducing Autophagic Cell Death through the Akt-TSC2-mTOR Signaling Pathway. *J. Mol. Cell Biol.* **2009**, *1*, 37–45.
21. Seleverstov, O.; Zabirnyk, O.; Zscharnack, M.; Bulavina, L.; Nowicki, M.; Heinrich, J. M.; Yezhelyev, M.; Emmrich, F.; O'Regan, R.; Bader, A. Quantum Dots for Human Mesenchymal Stem Cells Labeling. A Size-Dependent Autophagy Activation. *Nano Lett.* **2006**, *6*, 2826–2832.
22. Stern, S. T.; Zolnik, B. S.; McLeland, C. B.; Clogston, J.; Zheng, J.; McNeil, S. E. Induction of Autophagy in Porcine Kidney Cells by Quantum Dots: A Common Cellular Response to Nanomaterials? *Toxicol. Sci.* **2008**, *106*, 140–152.
23. Chen, Y.; Yang, L.; Feng, C.; Wen, L. P. Nano Neodymium Oxide Induces Massive Vacuolization and Autophagic Cell Death in Non-Small Cell Lung Cancer NCI-H460 Cells. *Biochem. Biophys. Res. Commun.* **2005**, *337*, 52–60.
24. Zabirnyk, O.; Yezhelyev, M.; Seleverstov, O. Nanoparticles as a Novel Class of Autophagy Activators. *Autophagy* **2007**, *3*, 278–281.
25. Osaki, F.; Kanamori, T.; Sando, S.; Sera, T.; Aoyama, Y. A Quantum Dot Conjugated Sugar Ball and Its Cellular Uptake. On the Size Effects of Endocytosis in the Subviral Region. *J. Am. Chem. Soc.* **2004**, *126*, 6520–6521.
26. Lu, F.; Wu, S. H.; Hung, Y.; Mou, C. Y. Size Effect on Cell Uptake in Well-Suspended, Uniform Mesoporous Silica Nanoparticles. *Small* **2009**, *5*, 1408–1413.
27. Chithrani, B. D.; Ghazani, A. A.; Chan, W. C. Determining the Size and Shape Dependence of Gold Nanoparticle Uptake into Mammalian Cells. *Nano Lett.* **2006**, *6*, 662–668.
28. Jiang, W.; Kim, B. Y.; Rutka, J. T.; Chan, W. C. Nanoparticle-Mediated Cellular Response Is Size-Dependent. *Nat. Nanotechnol.* **2008**, *3*, 145–150.
29. Shan, Y.; Ma, S.; Nie, L.; Shang, X.; Hao, X.; Tang, Z.; Wang, H. Size-Dependent Endocytosis of Single Gold Nanoparticles. *Chem. Commun.* **2011**, *47*, 8091–8093.
30. Chithrani, B. D.; Chan, W. C. Elucidating the Mechanism of Cellular Uptake and Removal of Protein-Coated Gold Nanoparticles of Different Sizes and Shapes. *Nano Lett.* **2007**, *7*, 1542–1550.
31. Wang, S. H.; Lee, C. W.; Chiou, A.; Wei, P. K. Size-Dependent Endocytosis of Gold Nanoparticles Studied by Three-Dimensional Mapping of Plasmonic Scattering Images. *J. Nanobiotechnol.* **2010**, *8*, 33.
32. Mizushima, N.; Yoshimori, T. How To Interpret LC3 Immunoblotting. *Autophagy* **2007**, *3*, 542–545.
33. Bjorkoy, G.; Lamark, T.; Brech, A.; Outzen, H.; Perander, M.; Overvatn, A.; Stenmark, H.; Johansen, T. P62/SQSTM1 Forms Protein Aggregates Degraded by Autophagy and Has a Protective Effect on Huntingtin-Induced Cell Death. *J. Cell Biol.* **2005**, *171*, 603–614.
34. Parkinson-Lawrence, E. J.; Shandala, T.; Prodoehl, M.; Plew, R.; Borlace, G. N.; Brooks, D. A. Lysosomal Storage Disease: Revealing Lysosomal Function and Physiology. *Physiology* **2010**, *25*, 102–115.
35. Vazquez, C. L.; Colombo, M. I. Assays To Assess Autophagy Induction and Fusion of Autophagic Vacuoles with a Degradative Compartment, Using Monodansylcadaverine (MDC) and DQ-BSA. *Methods Enzymol.* **2009**, *452*, 85–95.
36. Trombetta, E. S.; Ebersold, M.; Garrett, W.; Pypaert, M.; Mellman, I. Activation of Lysosomal Function during Dendritic Cell Maturation. *Science* **2003**, *299*, 1400–1403.
37. Christensen, K. A.; Myers, J. T.; Swanson, J. A. pH-Dependent Regulation of Lysosomal Calcium in Macrophages. *J. Cell Sci.* **2002**, *115*, 599–607.
38. Nakashima, S.; Hiraku, Y.; Tada-Oikawa, S.; Hishita, T.; Gabazza, E. C.; Tamaki, S.; Imoto, I.; Adachi, Y.; Kawanishi, S. Vacuolar H+-ATPase Inhibitor Induces Apoptosis *via* Lysosomal Dysfunction in the Human Gastric Cancer Cell Line MKN-1. *J. Biochem.* **2003**, *134*, 359–364.
39. Tietz, P. S.; Yamazaki, K.; LaRusso, N. F. Time-Dependent Effects of Chloroquine on pH of Hepatocyte Lysosomes. *Biochem. Pharmacol.* **1990**, *40*, 1419–1421.
40. Poole, B.; Ohkuma, S. Effect of Weak Bases on the Intralysosomal pH in Mouse Peritoneal Macrophages. *J. Cell Biol.* **1981**, *90*, 665–669.
41. Eto, K.; Yamashita, T.; Hirose, K.; Tsubamoto, Y.; Ainscow, E. K.; Rutter, G. A.; Kimura, S.; Noda, M.; Iino, M.; Kadowaki, T. Glucose Metabolism and Glutamate Analog Acutely Alkalinize PH of Insulin Secretory Vesicles of Pancreatic Beta-Cells. *Am. J. Physiol.* **2003**, *285*, E262–E271.
42. Gulbins, E.; Teichgraber, V.; Ulrich, M.; Endlich, N.; Riethmuller, J.; Wilker, B.; De Oliveira-Munding, C. C.; van Heeckeren, A. M.; Barr, M. L.; von Kurthy, G.; *et al.* Ceramide Accumulation Mediates Inflammation, Cell Death and Infection Susceptibility in Cystic Fibrosis. *Nat. Med.* **2008**, *14*, 382–391.
43. Forgac, M. Vacuolar ATPases: Rotary Proton Pumps in Physiology and Pathophysiology. *Nat. Rev. Mol. Cell Biol.* **2007**, *8*, 917–929.
44. Sumner, J. P.; Dow, J. A.; Earley, F. G.; Klein, U.; Jager, D.; Wieczorek, H. Regulation of Plasma Membrane V-ATPase Activity by Dissociation of Peripheral Subunits. *J. Biol. Chem.* **1995**, *270*, 5649–5653.
45. Ogata, M.; Hino, S.; Saito, A.; Morikawa, K.; Kondo, S.; Kanemoto, S.; Murakami, T.; Taniguchi, M.; Tanii, I.; Yoshinaga, K.; *et al.* Autophagy Is Activated for Cell Survival after Endoplasmic Reticulum Stress. *Mol. Cell. Biol.* **2006**, *26*, 9220–9231.
46. Kroemer, G.; Levine, B. Autophagic Cell Death: The Story of a Misnomer. *Nat. Rev. Mol. Cell Biol.* **2008**, *9*, 1004–1010.
47. Yorimitsu, T.; Klionsky, D. J. Eating the Endoplasmic Reticulum: Quality Control by Autophagy. *Trends Cell Biol.* **2007**, *17*, 279–285.
48. Mizushima, N. The Pleiotropic Role of Autophagy: From Protein Metabolism to Bactericide. *Cell Death Differ.* **2005**, *12*, 1535–1541.
49. Yang, Q.; She, H.; Gearing, M.; Colla, E.; Lee, M.; Shacka, J. J.; Mao, Z. Regulation of Neuronal Survival Factor MEF2D by Chaperone-Mediated Autophagy. *Science* **2009**, *323*, 124–127.
50. Guo, S.; Huang, Y.; Jiang, Q.; Sun, Y.; Deng, L.; Liang, Z.; Du, Q.; Xing, J.; Zhao, Y.; Wang, P. C.; *et al.* Enhanced Gene Delivery and SiRNA Silencing by Gold Nanoparticles Coated with Charge-Reversal Polyelectrolyte. *ACS Nano* **2010**, *4*, 5505–5511.

51. Kim, D.; Jeong, Y. Y.; Jon, S. A Drug-Loaded Aptamer-Gold Nanoparticle Bioconjugate for Combined CT Imaging and Therapy of Prostate Cancer. *ACS Nano* **2010**, *4*, 3689–3696.
52. Winchester, B.; Vellodi, A.; Young, E. The Molecular Basis of Lysosomal Storage Diseases and Their Treatment. *Biochem. Soc. Trans.* **2000**, *28*, 150–154.
53. Hwu, J. R.; Lin, Y. S.; Josephrajan, T.; Hsu, M. H.; Cheng, F. Y.; Yeh, C. S.; Su, W. C.; Shieh, D. B. Targeted Paclitaxel by Conjugation to Iron Oxide and Gold Nanoparticles. *J. Am. Chem. Soc.* **2009**, *131*, 66–68.
54. Javier, D. J.; Nitin, N.; Levy, M.; Ellington, A.; Richards-Kortum, R. Aptamer-Targeted Gold Nanoparticles as Molecular-Specific Contrast Agents for Reflectance Imaging. *Bioconjugate Chem.* **2008**, *19*, 1309–1312.
55. Clift, M. J.; Rothen-Rutishauser, B.; Brown, D. M.; Duffin, R.; Donaldson, K.; Proudfoot, L.; Guy, K.; Stone, V. The Impact of Different Nanoparticle Surface Chemistry and Size on Uptake and Toxicity in a Murine Macrophage Cell Line. *Toxicol. Appl. Pharmacol.* **2008**, *232*, 418–427.
56. Yu, T.; Malugin, A.; Ghandehari, H. Impact of Silica Nanoparticle Design on Cellular Toxicity and Hemolytic Activity. *ACS Nano* **2011**, *5*, 5717–5728.
57. Meerum Terwogt, J. M.; ten Bokkel Huinink, W. W.; Schellens, J. H.; Schot, M.; Mandjes, I. A.; Zurlo, M. G.; Rocchetti, M.; Rosing, H.; Koopman, F. J.; Beijnen, J. H. Phase I Clinical and Pharmacokinetic Study of PNU166945, a Novel Water-Soluble Polymer-Conjugated Prodrug of Paclitaxel. *Anticancer Drugs* **2001**, *12*, 315–323.
58. Wang, X.; Zhou, J.; Wang, Y.; Zhu, Z.; Lu, Y.; Wei, Y.; Chen, L. A Phase I Clinical and Pharmacokinetic Study of Paclitaxel Liposome Infused in Non-Small Cell Lung Cancer Patients with Malignant Pleural Effusions. *Eur. J. Cancer* **2010**, *46*, 1474–1480.
59. Frens, G. Controlled Nucleation for Regulation of Particle-Size in Monodisperse Gold Suspensions. *Nat. Phys. Sci.* **1973**, *241*, 20–22.
60. El-Sayed, M. A.; Link, S. Size and Temperature Dependence of the Plasmon Absorption of Colloidal Gold Nanoparticles. *J. Phys. Chem. B* **1999**, *103*, 4212–4217.